

Thiol-reactive Clenbuterol Analogues Conjugated to Bovine Serum Albumin

Marko Oblak^a, Andrej Preželj^c, Slavko Pečar^b, and Tom Solmajer^{a,c,*}

^a National Institute of Chemistry, Hajdrihova 19, SI-1001 Ljubljana, Slovenia.

Fax: +38614760300. E-mail: tom.solmajer@ki.si

^b Faculty of Pharmacy, University of Ljubljana, Aškerčeva 7, SI-1000 Ljubljana, Slovenia

^c Lek Pharmaceuticals d.d., Drug Discovery, Verovskova 57, SI-1526 Ljubljana, Slovenia

* Author for correspondence and reprint requests

Z. Naturforsch. **59c**, 880–886 (2004); received April 26/June 16, 2004

Several novel thiol-reactive clenbuterol analogues were coupled in high yield with bovine serum albumin (BSA). After labelling of unreacted cysteines with maleimide spin label (MiSL), the yield of the coupling reaction was determined by electron paramagnetic resonance (EPR) spectroscopy and spectral analysis. Two spin-probe populations with different mobility states were quantitatively determined. Molecular dynamics was used to model the structure of clenbuterol analogues and spin label conjugated to BSA and recognition of conjugates by anti-clenbuterol antibodies was demonstrated. The recognition of BSA-A, BSA-C and BSA-S conjugates with monoclonal and polyclonal anti-clenbuterol (mCLB-Ab and rCLB-Ab) antibodies was an indication, that chlorine substituents on the aromatic ring of clenbuterol derivatives are not necessary for the binding of antibodies to the conjugates. These results confirmed the importance of the *tert*-butylamino group as a part of the epitope and contribute to the understanding of the recognition process with anti-clenbuterol antibodies.

Key words: Clenbuterol, Electron Paramagnetic Resonance, Thiol Spin Labelling

Introduction

It is well-known that a number of β_2 -agonists have been used illegally at a higher dosage as a repartitioning agent in cattle feed, because they improve growth rate, reduce fat deposition and increase protein accretion. Clenbuterol has been reported as the most frequently used β_2 -agonist in function of an illegal “growth promoter” in several European countries. Considering the potential risk for human health, administration of β_2 -agonists to animals as repartitioning agents is banned within the European community (Directive 96/22/EC). Therefore the surveillance for the presence of residues of β_2 -agonists in meat and other edible tissues, as well as in living animals, is required for controls in all EU Member States (Blum and Flückiger, 1988; Butery and Sweet, 1993; Kuiper *et al.*, 1998).

The alerting reports of the widespread clenbuterol abuse prompted the development of new analytical procedures capable of screening and confirmation of a large range of various β_2 -agonists. For large-scale surveillance programs several methods have been used, including enzyme linked immunosorbent assay (ELISA) (Degand *et al.*, 1992; Petruzzelli *et al.*, 1996; Hahnau and Jülicher, 1996) and various techniques based on chromatography

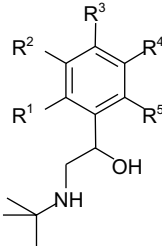
such as HPLC (Rashid *et al.*, 1999), LC-MS (Poletti *et al.*, 1995), GC-MS (Whaites and Murby, 1999) and GC with electron capture detection (van der Vlis *et al.*, 1995).

Commercially available antibodies have been raised against diazo-clenbuterol-BSA (bovine serum albumin) or salbutamol hemisuccinate-HRP (horseradish peroxidase) immunogens and have been found too specific for screening of structurally diverse β_2 -agonists with aromatic ring substituents R^1 – R^5 (Table I). The common feature of many β_2 -agonists is a 2-(*tert*-butylamino)-1-phenyl-1-ethanolic group. In an attempt to generalize the β_2 -agonists antigen epitope we designed and synthesized some novel thiol-reactive clenbuterol analogues, PA-S, PA-K, PA-A, and PA-C, without any substituents on the *ortho* positions of the aromatic ring and coupled them with a high yield to the unique free thiol group of BSA (Fig. 1) through their maleimido, iodoacetamido and acrylamido groups, respectively (Preželj and Pečar, 2002).

Furthermore, PA-K enables the coupling to the thiol group of BSA with the aliphatic amino group thus providing the assessment of the importance of the *tert*-butylamino epitope in the recognition process.

In this paper we describe how EPR spectroscopy was employed to quantify the yield of the

Table I. Chemical structures of some β_2 -agonists with a *tert*-butylamino group.



β_2 -agonist	R ¹	R ²	R ³	R ⁴	R ⁵
Clenbuterol	H	Cl	NH ₂	Cl	H
Salbutamol	H	CH ₂ OH	OH	H	H
Mabuterol	H	Cl	NH ₂	CF ₃	H
Bromobuterol	H	Br	NH ₂	Br	H
Terbutaline	H	OH	H	OH	H
Tolobuterol	H	H	H	H	Cl
Cimbuterol	H	CN	NH ₂	H	H
Carbuterol	H	NH-CO-NH ₂	OH	H	H

antigen coupling reaction to the thiol reactive group on the surface of BSA. The experimental spectra comprise of three spectral components arising from unbound residual MiSL and two motionally restricted covalently bound spin labels. Their contributions and characters were determined by spectral simulations and optimisation of the spectral parameters. At present the three-dimensional structure of BSA is not known. Recently, however, modelling of the proteolytic fragments and of the entire BSA structure has been reported (Curry *et al.*, 1999; Gelamo *et al.*, 2002). Encouraged by this and the fact that the high degree of homology between BSA and HSA (human serum albumin) suggests a very similar overall structure we modelled the structure of the synthesized thiol-reactive clenbuterol analogues conjugated to BSA and the structure of spin labelled BSA by using the resolved crystal structure of HSA (Bhattacharya *et al.*, 2000). Furthermore, molecular dynamics approach was used to model the spin-probe populations and compare the results with two different mobility states of nitroxide radicals as quantitatively determined by EPR spectroscopy.

We also describe the recognition of BSA conjugates with monoclonal and polyclonal anti-clenbuterol antibodies in a solid phase system.

Experimental

Materials and methods

The maleimide spin label MiSL (4-maleimido-1-oxy-2,2,6,6-tetramethylpiperidine) was prepared according to standard procedures (Berliner, 1976).

The clenbuterol analogues were synthesized according to the published procedure (Preželj and Pečar, 2002).

Coupling of thiol-reactive clenbuterol analogues PA-S, PA-A, PA-C and PA-K to BSA (corresponding conjugates BSA-S, BSA-A, BSA-C and BSA-K) and the labelling procedure of the conjugates with MiSL were described in detail by Preželj and Pečar (2002).

Monoclonal and polyclonal anti-clenbuterol (mCLB-Ab and rCLB-Ab) antibodies were kindly provided by Drs. M. Kane and C. Elliott.

Peroxidase-conjugated pig-anti rabbit immunoglobulins and peroxidase-conjugated rabbit-anti mouse immunoglobulins were purchased from DAKO, Carpinteria, CA, USA. 3,5,3',5'-Tetramethylbenzidine (TMB) and BSA were supplied by Sigma, Deisenhofen, Germany.

Modelling of BSA conjugates

The initial structures of the antigens MiSL, PA-A and PA-K were optimized using molecular mechanics as available in Spartan User Guide (2000). Monte Carlo approach was employed to search the conformational space due to flexible aliphatic bonds present in the clenbuterol analogues and the spin label molecule. The calculated conformations were superimposed to the conformer with the lowest energy and clustered into classes according to their geometry. Only one representative with the lowest energy of each class was chosen for further analysis. Subsequently, an initial model of BSA was obtained from the MODBASE database (Sánchez *et al.*, 2000) in which the sequence alignment with the human serum albumin and a three-dimensional template, the X-ray structure of HSA (PDB entry 1E7A, solved at a resolution of 2.2 Å) (Bhattacharya *et al.*, 2000) were used. The primary structure of the bovine protein from the SwissProt database (P02769) shares a 76% sequence identity with its human counterpart (P02768), what makes the model of BSA very reliable. The initial model of the conjugated proteins was built by forming a covalent bond of the ligands to the unique thiol group present on the BSA protein surface (Cys34)

using the program InsightII, Version 97 (InsightII User Guide, 1992). In order to relax any steric hindrances caused by this ligation, obtained conjugates were subjected to 100 ps of molecular dynamics (MD) simulations at a high temperature of 800 K, where only the ligand and residue Cys34 were allowed to move. The conformational features of BSA conjugates were subsequently analysed by MD and energy minimizations, using the program package CHARMM, Version c28c and the CHARMM22 empirical force field (Brooks *et al.*, 1983). A time step of 1 fs and Verlet algorithm were used during MD simulations. The non-bonded list was updated every 25 time steps and coordinates were written out every 100 fs. The dielectric constant was set to 1.0. Energy minimizations were performed using a combination of steepest descents and adopted basis Newton-Raphson methods and the minimization process was terminated when the energy gradients did not exceed 0.04 kJ/Å.

Conjugates with energy-minimized coordinates were then soaked with a 6.5 Å thick layer of water molecules and MD was performed for solvated conjugates. The first 30 ps of the dynamics were used for heating from 0 to 300 K and equilibration. Next, MD simulation was performed for 1 ns. During equilibration and dynamics of solvated conjugates only ligand atoms and all atoms (protein and solvent), which were less than 15 Å away from the ligand, were allowed to move. Finally, the structures obtained by 1 ns MD were averaged and subsequently minimized with a minimization algorithm as described above.

EPR spectroscopy and analysis

BSA was dissolved (0.335 g per 5 ml of buffer) in a phosphate buffer solution (100 mM sodium phosphate, pH 7.2, containing 1 g/l EDTA) and spin labelled with 0.7 equivalent of MiSL used as a thiol titrating agent. After spin labelling, the samples were measured in glass capillaries (1 mm inner diameter, volume range 20–40 µl) at 298 K. A Bruker CW-EPR ESP300E spectrometer operating at X-band (9.4 GHz) was utilised in our investigations. The spectral parameters were as follows: microwave power 20 mW, modulation amplitude 0.1 mT, modulation frequency 100 kHz, and scan range 10 mT. Temperature was controlled within 0.3 °C by the nitrogen stream system (Bruker). EPR data were acquired and analysed

using the supplied software. The experimental spectra were simulated with the EPRSIM 4.7 program and the calculated spectra were fitted to experimental ones using hybrid evolutionary and simplex optimisation methods (Štrancar *et al.*, 2000; Filipič and Štrancar, 2001).

Evaluation of antibody binding to BSA conjugates of various clenbuterol derivatives

The microtiter plates were coated with 1 mg/ml of the conjugates BSA-A, BSA-C, BSA-K and BSA-S (200 µl/well) in carbonate buffer, pH 9.6, for 1.5 h at 310 K. In case of the blank sample 1 mg/ml BSA was added instead of BSA conjugates (200 µl/well). After washing, 1/1000 dilution of monoclonal anti-clenbuterol (mCLB-Ab) and polyclonal anti-clenbuterol antibodies (rCLB-Ab) were added (200 µl/well) and incubated for 1 h at 310 K. The plates were again washed and 1/5000 dilution (200 µl/well) of pig-anti rabbit Ab-HRP (for rCLB-Ab) and rabbit-anti mouse Ab-HRP (for mCLB-Ab) were added and incubated for 1 h at 310 K. After the washing step, 200 µl of TMB were added for 30 min at room temperature. The reaction was stopped with 1 M H₂SO₄ and the absorbance was measured at 450 nm.

Results and Discussion

The primary structure of BSA consists of 577 amino acid residues, 35 of them are cysteines, 34 cysteine residues form disulphide bridges and there is only one 'free' cysteine residue, Cys34, which is located in the crevice on the protein surface of domain I. The ligands react with the unique free thiol group of residue Cys34 of the BSA protein molecule and form a covalent bond.

They were preferentially titrated with 0.7 equivalent of the thiol-specific maleimide spin label MiSL (Fig. 1). On the basis of measurements performed with intact BSA the presence of 0.62 modified thiols per BSA molecule was revealed. This result is in a close agreement with the published data (0.6–0.7 mol SH-groups/mol BSA) (Peters, 1985).

As compared with the characteristic sharp three-line pattern EPR spectrum of MiSL tumbling in solution, a new component in the low field region occurred. The observed EPR spectrum (Fig. 2) can be regarded as a superimposition of spectrum from unbound, residual MiSL (component 1) and

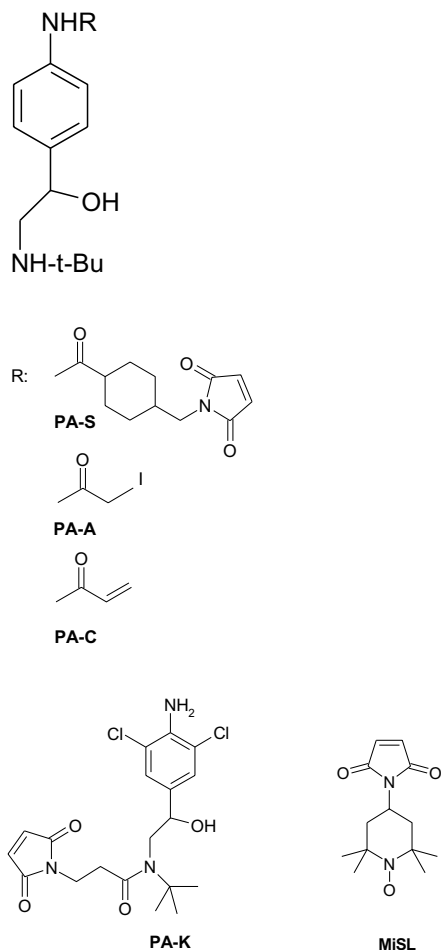


Fig. 1. β_2 -Agonists antigen and chemical structures of thiol-reactive ligands: (\pm) -*N*-[4-[2-(*tert*-butylamino)-1-hydroxyethyl]phenyl-2-iodo]acetamide (PA-A), (\pm) -*N*-[4-[2-(*tert*-butylamino)-1-hydroxyethyl]phenyl]acrylamide (PA-C), (\pm) -*N*-[4-[2-(*tert*-butylamino)-1-hydroxyethyl]phenyl]-4-[(2,5-dioxo-2,5-dihydro-1*H* pyrrol-1-yl) methyl] cyclohexanecarboxamide (PA-S), and (\pm) -*N*-[2-(4-amino-3,5-dichlorophenyl)-2-hydroxyethyl]-*N*-(*tert*-butyl)-3-(2,5-dioxo-2,5-dihydro-1*H*-pyrrol-1-yl) propanamide (PA-K) and of the spin label MiSL.

motionally restricted EPR spectra of the covalently attached spin labels (components 2, 3).

The proportions of the components 1, 2 and 3 have been quantitatively determined from the calculated EPR spectra fitted to the experimental ones with the EPRSIM 4.7 program. The calculated spectra revealed the relative populations between bound and free MiSL and allowed us to estimate the rotational parameters for each of the fitted components and the yield of the coupling

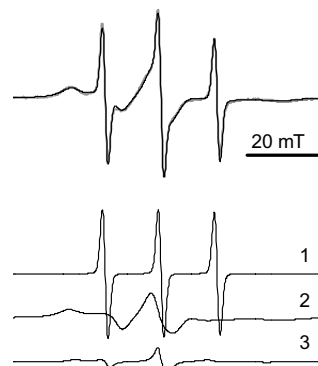


Fig. 2. The total simulated spectrum (black line) fitting well with the experimental spectrum (gray line) (top) is shown together with three components representing residual MiSL (1), strongly immobilized (2) and weakly immobilized spin label (3) (bottom).

reaction. The proportion of MiSL with pronounced mobility restrictions is $89.1 (\pm 1)\%$, whereas the proportion of unbound spin probe tumbling in solution is $10.9 (\pm 1)\%$. Assuming that the unspecific binding is rather low and knowing the proportion of residual MiSL in buffer, the yield of the coupling reaction for BSA conjugates was derived from the simulated spectrum.

The EPR spectrum of spin labelled BSA is characterized by the coexistence of two spectral components, indicating the presence of two spin-probe populations with different mobility states. A component in the low field region corresponds to the strongly immobilized signal [population proportion of $80.8 (\pm 6)\%$ and correlation time $\tau_c = 1.7 (\pm 2)$ ns] reflecting the spin label restricted in its local motion. Whereas the weakly immobilized component [population proportion of $8.3 (\pm 6)\%$ and correlation time $\tau_c = 0.3 (\pm 1)$ ns] has the same isotropic hyperfine splitting as residual MiSL tumbling in buffer, which indicates the hydrophilic character of the local environment around the cysteine residue. The covalent binding of MiSL to the cysteine residues of BSA can be observed in the overlapping central region as the higher intensity ratio between the high- and low-field lines for the weakly immobilized component (Houstek *et al.*, 1983; Alonso *et al.*, 2000).

The molecular motion of MiSL covalently bound to BSA was restricted to different degrees on the time scale of EPR spectroscopy. The weakly immobilized component was considered to have nearly isotropic motion with a slight decrease in

mobility compared with that for the label tumbling in solution (τ_c around 0.06 ns). Two different mobility states of covalently attached MiSL were confirmed also with calculated correlation times τ_c (between 1.7 and 0.3 ns) for spectral components derived from simulated spectra.

A difference in the mobility of bound MiSL could be the result of different accessibility of the nitroxide radical to the Cys34 located in a BSA cleft or pocket. In that case the local environment greatly restricts the motion of the bound probe and prevents its re-orientation around the bonds that link the maleimide label to the protein.

Two spectral components could be also explained by the fact that a portion of covalently bound MiSL is hydrogen-bonded to BSA amino acid residues in the vicinity of the site of attachment and another portion exposed to the aqueous environment. In that case the formation of hydrogen bonds would lead to a strongly immobilized component, whereas the weakly immobilized signal might reflect the spin label bound to the more accessible non-hydrogen bonded external site in contact with the aqueous environment.

Conformational analysis of MiSL and molecular dynamics results of simulations performed on the BSA-MiSL system corroborate these findings.

Conformational analysis revealed that MiSL is conformationally restricted to two conformers: MiSL-1 described by a dihedral angle $\theta = -132^\circ$ (*i.e.* the piperidine ring is roughly perpendicular to the maleimido moiety) and MiSL-2 with a dihedral angle $\theta = -30^\circ$.

Energetically speaking, the conformer MiSL-1 has a 42 kJ/mol lower energy than MiSL-2. In contrast, the conformational analysis of PA-A and PA-K ligands resulted in 32 and 98 conformations, respectively.

For MiSL-1 conjugated to the Cys34 of BSA a hydrogen bond can be observed between one of the carbonyl oxygen atoms of MiSL-1 and the hydroxyl group of residue Thr83 (distance between carbonyl and hydroxyl oxygen is 2.9 Å, O...H-O angle is 158.6°). In contrast, MiSL-2 forms no direct hydrogen bond(s) with BSA (corresponding distance and angle are 6.4 Å and 141.2°, respectively). In Fig. 3, a part of the average structure of the BSA protein conjugated with MiSL-1 is shown.

Also the binding pocket of MiSL-2 is more exposed to the solvent compared to the binding pocket of MiSL-1. Furthermore, in the case of

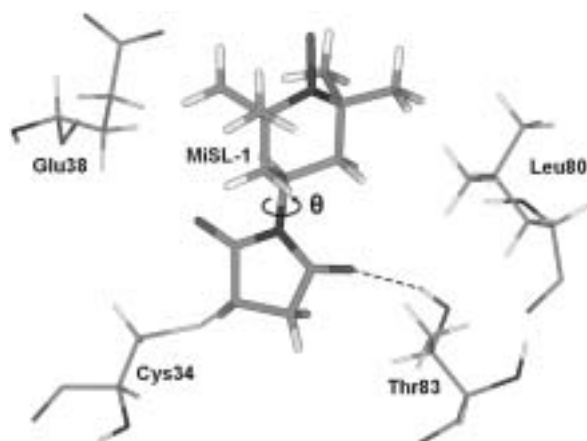


Fig. 3. Spin label MiSL-1 conjugated to Cys34 of BSA. In conformation denoted MiSL-1 is hydrogen bonded (dashed line) to hydroxyl group of the Thr83 amino acid side chain.

MiSL-1 hydrophobic interactions between the alkyl region of side chain Glu38 and methyl groups of MiSL-1 act favourably to lower the energy. In contrast, Leu80 side chain provides hydrophobic interactions with the piperidine moiety in both BSA-MiSL-1 and BSA-MiSL-2 conjugates. As a consequence, this could be interpreted as the reason for a restricted motion in case of MiSL-1 observed in the EPR spectra while in case of MiSL-2 the motion is not hindered.

Recognition of our BSA conjugates was determined with monoclonal and polyclonal anti-clenbuterol antibodies (mCLB-Ab and rCLB-Ab). The binding of the antibodies to BSA conjugates of various clenbuterol derivatives was evaluated in a solid phase system (Fig. 4).

Direct conjugation of a small ligand can lead to loss of an antigenic determinant and shielding of the ligand by the steric bulk of the carrier protein. Therefore an appropriate spacer group that enlarges the ligand/protein distance was introduced.

The molecular dynamics simulations revealed how the clenbuterol analogues project into space for binding to antibody.

Binding of monoclonal and polyclonal anti-clenbuterol antibodies to the immobilized BSA conjugates was detected with secondary antibodies coupled with horseradish peroxidase. In case of the blank sample there was no colour change after adding the substrate. The BSA-A, BSA-C and BSA-S conjugates were recognized by both mCLB-Ab and rCLB-Ab (Table II).

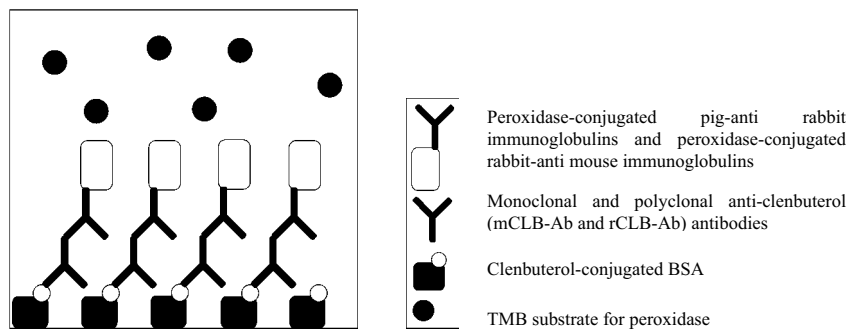


Fig. 4. Binding of monoclonal and polyclonal anti-clenbuterol (mCLB-Ab and rCLB-Ab) antibodies to the immobilized BSA conjugates. 3,5,3',5'-Tetramethylbenzidine (TMB) substrate for horseradish peroxidase.

Table II. Binding of mCLB-Ab and rCLB-Ab to BSA conjugates. Absorbance change at 450 nm was measured.

BSA conjugate	A_{450} for mCLB-Ab	A_{450} for rCLB-Ab
BSA-A	3.46	0.81
BSA-C	2.30	0.39
BSA-S	2.56	0.23
BSA-K	0	0

The BSA-K was not recognized by either antibody. These results were as expected as, in BSA-K, the thiol-reactive moiety is attached to the aliphatic amino group, which is supposed to be a part of epitope and the immunogen conjugates are prepared by diazotization.

Interestingly, a clue to the variable antibody binding observed in the case of BSA-A and BSA-K can be found in MD simulations. The BSA-K conjugate, for which no antibody binding could be observed despite the presence of a β_2 -agonist moiety in the hapten structure, has a *tert*-butylamino group also projected into the space available for antibody recognition, as observed in the BSA-A conjugate. However, the preferred conformation of the whole ligated PA-K structure, which does not allow the antibody to access the part of the hapten necessary for recognition is due to the flexibility of the spacer between the malei-

mido moiety and the phenyl ring and interactions of PA-K with BSA protein surface,

The spectral analysis of site-directed spin labeling using simulation and decomposition of the spectra is a powerful tool for a more quantitative description of the dynamic modes of the nitroxide side chains. Two different mobility states of covalently attached MiSL were revealed, which could be the result of different accessibility of probe to the cysteine residue. The use of molecular dynamics provided a plausible interpretation of these data: besides the steric hindrance due to the local environment, the two motionally restricted spectral components could be explained also by preferential formation of hydrogen bonds.

Acknowledgements

We are thankful to Drs. M. Kane (Bioresearch, National Diagnostics Center, Galloway, Ireland) and C. Elliott (Department of Agriculture for Northern Ireland, University of Northern Ireland) for kindly providing the polyclonal antiserum and help in developing the immunoassay. We are indebted to the European Commission (Brussels, Belgium) and the Ministry of Education, Science and Sport (Ljubljana, Slovenia) for financial assistance. We also thank the Institute Jožef Stefan (Ljubljana, Slovenia) for the use of their instrument facilities and Professor R. Pain (Ljubljana, Slovenia) for the revision of the manuscript.

- Alonso A., dos Santos J. G., and Tabak M. (2000), *Stratum corneum* protein mobility as evaluated by a spin label maleimide derivative. *Biochim. Biophys. Acta* **1478**, 89–101.
- Berliner L. J. (1976), Spin Labelling. Theory and Applications. Academic Press, London, pp. 213–214.
- Bhattacharya A. A., Curry S., and Franks N. P. (2000), Binding of the general anesthetics propofol and halothane to human serum albumin. High resolution crystal structures. *J. Biol. Chem.* **275**, 38731–38738.
- Blum J. W. and Flückiger N. (1988), Early metabolic and endocrine effects of perorally administered β -adrenoceptor agonists in calves. *Eur. J. Pharmacol.* **151**, 177–178.
- Brooks B. R., Bruccoleri R. E., Olafson B. D., States D. J., Swaminathan S., and Karplus M. (1983), CHARMM: A program for macromolecular energy, minimization and dynamics calculations. *J. Comp. Chem.* **4**, 187–271.
- Butery P. J. and Sweet A. (1993), Manipulation of lean deposition in animals. *Anim. Feed Sci. Tech.* **45**, 97–115.
- Curry S., Brick P., and Franks N. P. (1999), Fatty acid binding to human serum albumin: new insights from crystallographic studies. *Biochim. Biophys. Acta* **1441**, 131–140.
- Degand G., Bernes-Duyckaerts A., and Maghuin-Rogister G. (1992), Determination of clenbuterol in bovine tissues and urine by enzyme immunoassay. *J. Agric. Food Chem.* **40**, 70–75.
- Filipič B. and Štrancar J. (2001), Tuning EPR spectral parameters with a genetic algorithm. *Appl. Soft. Comput.* **1**, 83–90.
- Gelamo E. L., Silva C. H. T.P., Imasato H., and Tabak M. (2002), Interaction of bovine (BSA) and human (HSA) serum albumins with ionic surfactants: spectroscopy and modelling. *Biochim. Biophys. Acta* **1594**, 84–99.
- Hahnau S. and Jülicher B. (1996), Evaluation of commercially available ELISA test kits for the detection of clenbuterol and other β_2 -agonists. *Food Addit. Contam.* **13**, 259–273.
- Houstek J., Bertoli E., Stipani I., Pavelka S., Megli F. M., and Palmieri F. (1983), Characterisation of sulphhydryl groups of the mitochondrial phosphate translocator by a maleimide spin label. *FEBS Lett.* **154**, 185–190.
- InsightII User Guide (1992), Version 2.1.0. San Diego, Biosym Technologies.
- Kuiper H. A., Noordam M. Y., van Dooren-Flipsen M. M. H., Schilt R., and Roos A. H. (1998), Illegal use of β -adrenergic agonists: European Community. *J. Anim. Sci.* **76**, 195–207.
- Peters T. Jr. (1985), Serum albumin. *Adv. Prot. Chem.* **37**, 161–245.
- Petruzzelli E., Ius A., Berta S., Dovis M., and Albertini A. (1996), Preparation and characterization of a monoclonal antibody specific for the β -agonist clenbuterol. *Food Agric. Immunol.* **8**, 3–10.
- Polettini A., Montagna M., Hogendoorn E. A., Dijkman E., van Zoonen P., and van Ginkel L. A. (1995), Applicability of coupled-column liquid chromatography to the analysis of β -agonists in urine by direct sample injection. *J. Chromatogr. A* **695**, 19–31.
- Preželj A. and Pečar S. (2002), Synthesis of novel thiol-reactive clenbuterol analogues. *Pharmazie* **57**, 70–71.
- Rashid B. A., Kwasowski P., and Stevenson D. (1999), Solid phase extraction of clenbuterol from plasma using immunoaffinity followed by HPLC. *J. Pharm. Biomed. Anal.* **21**, 635–639.
- Sánchez R., Pieper U., Mirkovic N., deBakker P. I. W., Wittenstein E., and Sali A. (2000), MODBASE, a database of annotated comparative protein structure models. *Nucl. Acids Res.* **28**, 250–253.
- Spartan User Guide (2000), Version 5.0. Wavefunction Inc., Irvine, CA.
- Štrancar J., Šentjerc M., and Schara M. (2000), Fast and accurate characterisation of biological membranes by EPR spectral simulations of nitroxides. *J. Mag. Res.* **142**, 254–265.
- van der Vlis E., Mazereeuw M., Tjaden U. R., Irth H., and van der Greef J. (1995), Rapid analysis of β -agonists in urine by thermospray tandem mass spectrometry. *J. Chromatogr. A* **712**, 227–234.
- Whaites L. X. and Murby E. J. (1999), Determination of clenbuterol in bovine urine using gas chromatography-mass spectrometry following clean-up on an ion-exchange resin. *J. Chromatogr.* **728**, 67–69.